UNIVERSITAT DE BARCELONA

ICFO

MASTER THESIS

NONLOCALITY IN QUANTUM NETWORKS: CHARACTERIZING THE BILOCAL CORRELATIONS

Institute of Photonic Sciences (ICFO)

Group of Quantum Information

María Ciudad Alañón

Supervisors: **Paolo Abiuso and Marc-Olivier Renou**

11 July 2022

Bell's theorem proved that quantum theory cannot be fully explained with local hidden variable models. This led to the emergence of the field of nonlocality, which has been generalized to more sophisticated scenarios than the standard Bell scenario, called network scenarios. This thesis focuses on the characterization of the correlations in the simplest nontrivial bilocal scenario. While correlations in the standard Bell scenario form a convex set, in networks the set of correlations is non-convex, making the problem challenging. We construct an oracle that tells us whether a correlation is bilocal or not. We study analytically the geometry of the bilocal set. Finally, we describe two different ways of generating nonlocality and give a intuition of what is genuinely nonbilocal.

Acknowledgements

I would like to thank my supervisor Paolo Abiuso who has been a great tutor and a great source of learning, as well as giving me all the time I needed. Furthermore, I would like to thank Emanuel-Cristian Boghiu for his contributions and time dedicated to collaborate. Also, I appreciate some fruitful discussions with Marc-Olivier Renou. Finally, I would like to give my great appreciation to ICFO and, in particular, the Quantum Information group led by Antonio Acín for giving me the opportunity to do the work in such a good environment and surrounded by so many talented people.

Contents

1 INTRODUCTION **1**
- 1.1 BELL SCENARIO . . . 1
- 1.2 BEYOND THE STANDARD BELL SCENARIO:NETWORKS . . . 3
- 1.3 BILOCAL NETWORK . . . 4
- 1.4 SUMMARY OF THE CONTRIBUTIONS . . . 5

2 BILOCAL ORACLE **6**
- 2.1 THEORY OF THE ORACLE . . . 6
- 2.2 IMPLEMENTATION AND TESTS . . . 9

3 ANALYSIS OF THE BILOCAL SET **11**
- 3.1 UNDERSTANDING THE GEOMETRY OF THE SET . . . 11
  - 3.1.1 Disproving the conjecture . . . 14
- 3.2 GENUINE NONLOCALITY . . . 16
  - 3.2.1 Entanglement-swapping . . . 17
  - 3.2.2 Fritz argument . . . 17
  - 3.2.3 Mixing cheating scenarios . . . 18

4 CONCLUSION **19**

References **20**

A Proof of the CHSH inequality **21**

B Maximal violation of the CHSH **21**

C Pictorial representation of the conditions on Bob's outputs **23**

D Pictorial representation when Bob has 3 outputs **24**

E Elegant Joint Measurment **24**

F Proof lemma 3.1 **25**

G Proof lemma 3.2 **25**

H Proof of lemma 3.3 **26**

1 INTRODUCTION

In 1935 a paper was published by Einstein, Podolsky and Rosen (EPR) that sparked a debate on the completeness of quantum theory viewed as a local-realistic (LR) model [EPR35]. According to this paper, any physical theory has to satisfy:

- Locality, in the sense that there cannot be a causal relationship between space-like separated events.
- Reality: it must be possible to predict a physical quantity with certainty without disturbing the system.
- Completeness, i.e., every element of the physical reality must have a counterpart in the physical theory.

In 1964, J. Bell published a paper ending the debate. In it, he formalized the conditions that must be fulfilled by any local hidden variable theory and proposed an experiment that was quantum in nature and violated these conditions [Bel64]. These conditions are the so-called Bell inequalities. The first experimental violations of Bell inequalities ([AGR81] and [TBZG98] among others) put an end to the EPR conflict.

Bell established a theorem according to which no physical theory based solely on local variables can fully explain all the quantum theory predictions. Because of it, in recent years, research has been developed in the nonlocality field [BCP+14]. Its relevance is two-fold. First, from the foundational point of view to understand quantum theory in scenarios such as those proposed by Bell and in more sophisticated ones. Second, developing quantum information theory to use it in networks towards information processing tasks leading to different applications such as the quantum Internet or quantum cryptography [BCP+14, TPKR+21].

1.1 BELL SCENARIO

The standard Bell scenario consists of several non-communicating observers measuring in their respective shares of a system emitted by a single physical source. Consider two observers, Alice (A) and Bob (B). They can choose which measurement they perform, labelled as x and y, respectively, and they can obtain different outcomes, respectively denoted a and b [TPKR+21] (Fig. 1). If the experiment is repeated many times, we will

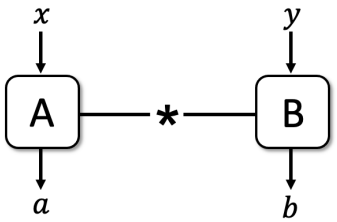

Figure 1: Representation of the standard (bipartite) Bell scenario

obtain the relative frequencies of (a, b) given (x, y). This will result in a probability distribution $p(a, b|x, y)$, which is the correlation shared by the parties A and B. A correlation is local, i.e., it satisfies Bell's local causality assumption, if it can be written as:

$$p(ab|xy) = \int d\lambda \mu(\lambda) p_A(a|x\lambda) p_B(b|y\lambda), \tag{1}$$

where λ, the so-called hidden variable, contains all the information about the common past of the shares and it is subject to some unknown probability density $\mu(\lambda)$. Note that Alice's and Bob's inputs are independent from the hidden variable ($\mu(\lambda|x,y) = \mu(\lambda)$) [TPKR+21].

The output of each party does not depend on the input of the other one. This assumption is called the no-signaling principle (NS) and it is written as

$$\begin{aligned} \forall b,x,y: \quad & \sum_a p(a,b \mid x,y) = p(b \mid x,y) \overset{\text{NS}}{=} p(b \mid y), \\ \forall a,x,y: \quad & \sum_b p(a,b \mid x,y) = p(a \mid x,y) \overset{\text{NS}}{=} p(a \mid x). \end{aligned} \tag{2}$$

The set of correlations that satisfy the NS principle, $\mathcal{NS}$, strictly contains the set of local correlations, $\mathcal{L}$. If the number of inputs and outputs is finite, $\mathcal{L}$ can be characterized in terms of a polytope known as the local polytope. Without loss of generality, the response functions p_A and p_B can be assumed to be deterministic functions (they provide output in function of the inputs and the hidden variable λ), as any randomness in them can be absorbed in $\mu(\lambda)$. Because of that, each deterministic function corresponds to a vertex of the polytope. Moreover, we can set λ to belong to a finite set and, then, replace the integral by a summation because, as the number of inputs and outputs is finite, the number of deterministic responses is also finite. The local correlations form a local polytope as they are convex combination of the vertices because of the freedom of varying $\mu(\lambda)$. The facets of the polytope can be determined and correspond to the Bell inequalities (Fig. 2). Hence, one can infer if a correlation is local or not by checking if all these inequalities are or not satisfied, respectively. The violation of one Bell inequality is sufficient to determine that a correlation is nonlocal [TPKR+21].

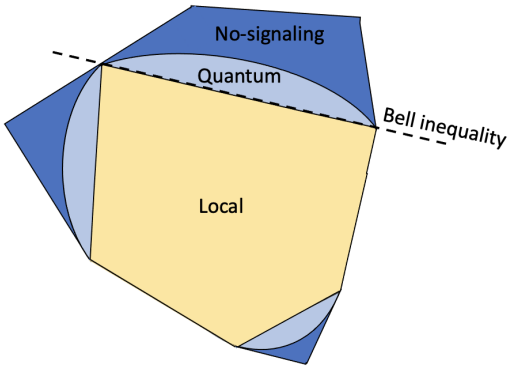

Figure 2: Representation of the local, quantum and no-signalling set.

The simplest and best known Bell inequality is the Clauser-Horne-Shimony-Holt (CHSH) Bell inequality [CHSH69]. Let's consider a scenario with 2 parties which have binary inputs $x, y \in \{0,1\}$ and binary outputs $a, b \in \{-1,+1\}$. The inequalities that represent the non-trivial facets of the polytope can be written as:

$$S_{CHSH} = \langle A_0 B_0 \rangle + \langle A_0 B_1 \rangle + \langle A_1 B_0 \rangle - \langle A_1 B_1 \rangle \leq 2, \tag{3}$$

up to relabellings, with $\langle A_x B_y \rangle = \sum_{a,b} a \cdot b \cdot p(a,b|x,y)$ (proof in Appendix A).

To see a violation of the CHSH inequality, imagine that A and B share $|\phi^+\rangle = \frac{1}{\sqrt{2}}(|00\rangle + |11\rangle)$ (the maximally entangled state) and that A and B performs the following measurements: $A_1 = \sigma_x$, $A_2 = \sigma_z$, $B_1 = (\sigma_x + \sigma_z)/\sqrt{2}$ and $B_2 = (\sigma_x - \sigma_z)/\sqrt{2}$. These conditions make $S_{CHSH} = 2\sqrt{2} > 2$. Indeed, $2\sqrt{2}$ corresponds to the maximal violation of

the CHSH [Cir80] (proof in Appendix B). The first experimental verification of a CHSH violation was in 1972 [FC72].

It is important to notice that the CHSH inequality can be violated in quantum theory, in which the correlations are given by the Born rule [TPKR+21]:

$$p(a,b|x,z) = Tr(A_{a|x} \otimes B_{b|y} \cdot \rho), \tag{4}$$

where $\{A_{a|x}\}$ and $\{B_{b|y}\}$ are measurements acting on $\mathcal{H}_A$ and $\mathcal{H}_B$, respectively, and ρ, a quantum state acting on $\mathcal{H}_A \otimes \mathcal{H}_B$. These form the set $\mathcal{Q}$, which satisfies No-Signalling and which strictly contains $\mathcal{L}$ (see Fig. 2).

1.2 BEYOND THE STANDARD BELL SCENARIO:NETWORKS

The study of nonlocality can be extended to the multipartite Bell case in which more than two parties are connected to one source (Fig. 3a). Moreover, in recent years, nonlocality has been extended to the case of generic networks, whose difference with respect to the former is the presence of more than one source. These sources are assumed to be independent between them and that independence is translated into the association of a hidden variable to each source. Each source gives a share of a physical system to some parties of the network. Hence, each party can receive one or more shares from different sources [TPKR+21].

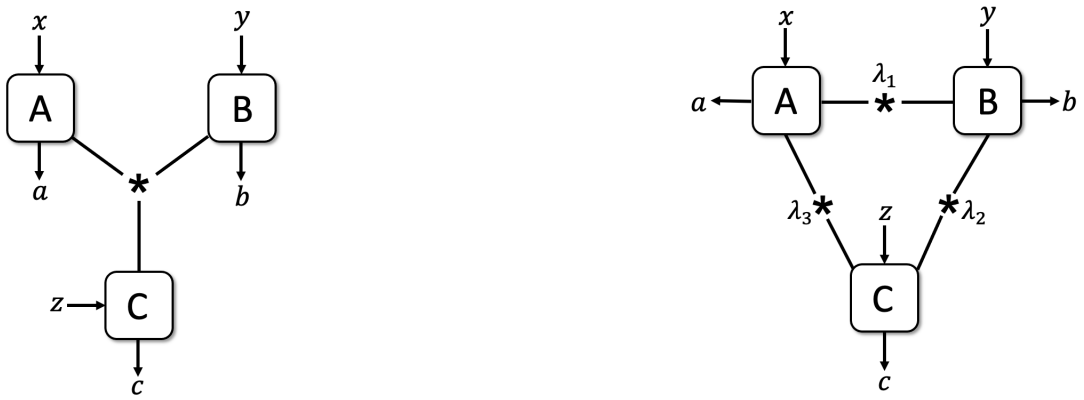

Figure 3: Representation of the Bell scenario with three parties (a) and the triangle network (b).

Generalizing Eq. (1), a correlation with m sources and n parties is local for a given network if it can be written as:

$$p(\bar{a}|\bar{x}) = \int d\lambda_1 \mu(\lambda_1) \cdots \int d\lambda_m \mu(\lambda_m) p_{A_1}(a_1|x_1\bar{\lambda}_1) \cdots p_{A_n}(a_n|x_n\bar{\lambda}_n), \tag{5}$$

where $\bar{a} = (a_1, ..., a_n)$ are the outputs of the n different parties given their inputs $\bar{x} = (x_1, ..., x_n)$ and $\bar{\lambda}_j$ corresponds to the set of the different hidden variables associated to the sources that send a share to the party j. In order to clarify this definition, let us consider one of the most studied networks which is the triangle network (Fig. 3b). This scenario gives a local correlation if it can be written as follows:

$$p(a,b,c|x,y,z) = \int d\lambda_1 \mu(\lambda_1) \int d\lambda_2 \mu(\lambda_2) \int d\lambda_3 \mu(\lambda_3) p_A(a|x,\lambda_1,\lambda_3) p_B(b|y,\lambda_1,\lambda_2) p_C(c|z,\lambda_2,\lambda_3). \tag{6}$$

The independence of the sources makes the set of local network correlations more complex than a polytope. The set of such correlations satisfies:

- It is inside the n-partite local polytope (Fig. 4a).
- It is nonconvex [BGP10].
- It is connected, closed and defined by a finite number of polynomial inequalities [Fri12].

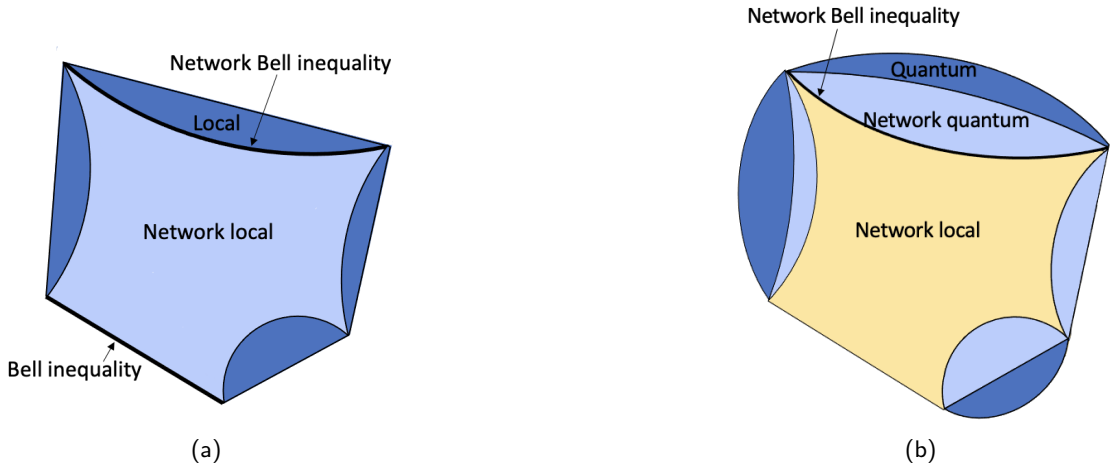

Figure 4: Representation of the local and quantum set. In the first image (a), the local set of the network within the local set is represented. In the second (b), the local set of the network is shown within the network quantum set which is in turn inside the quantum set.

In quantum networks, the independence of the sources is equivalent to have independent quantum states ρ_j. In that case, the correlations are:

$$p(\bar{a} \mid \bar{x}) = \mathrm{Tr}\left[\left(A^{(1)}_{a_1|x_1} \otimes \ldots \otimes A^{(n)}_{a_n|x_n}\right) \cdot (\rho_1 \otimes \ldots \otimes \rho_m)\right], \tag{7}$$

where $A^{(j)}_{a_j|x_j}$ is the measurement performed by the party j, and has support on the Hilbert space of each share of the ρ_i that is sent to party j. Analogous to the classical definition, let us consider the triangular network. The quantum correlations for this case are

$$p(a,b,c|x,y,z) = \mathrm{Tr}\left[\left(A^{(A_1A_2)}_{a|x} \otimes B^{(B_1B_2)}_{b|y} \otimes C^{(C_1C_2)}_{c|z}\right) \cdot \left(\rho_1^{(A_2B_1)} \otimes \rho_2^{(B_2C_1)} \otimes \rho_3^{(C_2A_1)}\right)\right], \tag{8}$$

where the respective Hilbert spaces are ordered according to the network configuration. Like the set of local network correlations, the set of quantum network correlations is closed and it is not convex. The quantum network correlation set contains the local network set but it is not contained in the Bell-local polytope (Fig. 4b) [TPKR$^+$21].

1.3 BILOCAL NETWORK

This work is focused on the study of the simplest quantum network which is the bilocal network. This scenario is very interesting, not only from a fundamental perspective, but also from a quantum information point of view in which the understanding of this network

might help in designing protocols for the use of quantum phenomena, such us entanglement swapping, cryptography, and other information processing tasks.

This scenario consists of 3 parties on a line –Alice(A), Bob(B) and Charlie(C)– and two sources between Alice-Bob and Bob-Charlie. Each party receives an input (x, y and z, respectively) and gives an output (a, b and c), as it is shown in Fig. 5, thus giving rise to correlations of the form $p(a, b, c|x, y, z)$ [TPKR+21].

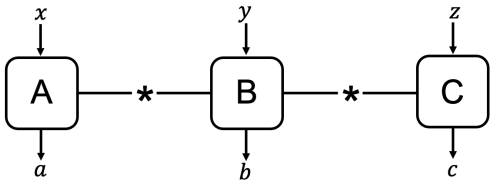

Figure 5: Representation of the bilocal scenario

The independence of the sources makes A and C uncorrelated, i.e., they are conditionally independent, which is rendered by

$$\sum_b p(a, b, c|x, y, z) = p(a, c|x, z) = p(a|x)p(c|z). \tag{9}$$

The correlation $p(a, b, c|x, y, z)$ admits a bilocal model, i.e., it admits a network local model, if it can be written as

$$p(a, b, c|x, y, z) = \int\int d\lambda_1 d\lambda_2 \mu(\lambda_1)\mu(\lambda_2) p_A(a|x, \lambda_1) p_B(b|y, \lambda_1, \lambda_2) p_C(c|z, \lambda_2). \tag{10}$$

Determining if a correlation is bilocal or not is nontrivial. There are some necessary but not sufficient inequalities for certain bilocal scenarios [BRGP12].

One of the phenomena that produces nonlocality in the bilocal scenario is the entanglement swapping[BGP10, BRGP12]. Such process makes it possible for two particles that have never interacted with each other to be nonlocally correlated [BGP10].

1.4 SUMMARY OF THE CONTRIBUTIONS

This section describes the work that has been done on this master thesis, which you will find in the following sections. Section 2, tells how an oracle has been obtained to determine whether a correlation is bilocal or not. In subsection 2.1, the problem to address this goal is presented and analytically characterized, while in subsection 2.2 we describe the implementation of the oracle via linear and bilinear optimization software, as well as various tests that were carried out for its verification. In section 3, the bilocal set is analysed. First, in section 3.1, we try to better understand its geometry by formulating a conjecture relating the bilocal set to standard Bell bipartite scenario, and testing its falsity. In section 3.2, we study different scenarios in which non-bilocality can be produced with quantum sources. Some of the bilocality violations can be directly related to an underlying bipartite nonlocality, therefore posing the question of what are the quantum phenomena that are "genuinely new" in the bilocal scenario. In addition, considering convex mixtures of these examples, we find quantumly feasible nonbilocal correlations that do not show straightforward hidden locality violation. Finally, the appendices contain technical details and derivations.

2 BILOCAL ORACLE

The main objective we address in this thesis is the characterization of the "easiest" nontrivial network that can exhibit nonlocality. Although simplicity is not a characteristic that can be quantified, we consider a minimal bilocal scenario which corresponds to the one in which Alice and Charlie have binary inputs ($x, z \in \{0, 1\}$) and everyone has binary outputs ($a, b, c \in \{0, 1\}$) (Fig.6).

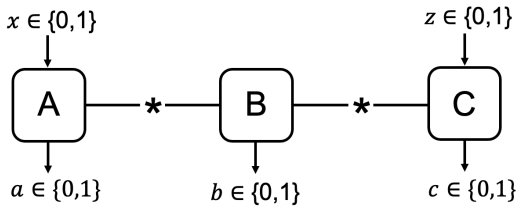

Figure 6: Representation of the simplest bilocal scenario

2.1 THEORY OF THE ORACLE

The correlation $p(a, b, c|x, z)$ will be bilocal if it can be written as Eq. (10). The response functions in it can be assumed to be deterministic, as any randomness in them can be absorbed in $\mu(\lambda_1)$ and $\mu(\lambda_2)$. Furthermore, λ_1 and λ_2 can be taken as flat distributions from 0 to 1 (then, $\mu(\lambda_1) = 1 = \mu(\lambda_2)$), by rescaling the response function of each party. Hence, the bilocal equation (Eq. (10)) becomes:

$$p(a, b, c|x, y, z) = \int_0^1 \int_0^1 d\lambda_1 d\lambda_2 p_A(a|x, \lambda_1) p_B(b|\lambda_1, \lambda_2) p_C(c|z, \lambda_2). \tag{11}$$

This means that correlations can be represented in a square as it is showed in Fig. 7a. Moreover, λ_1 and λ_2 are taken to be between 0 and 1 and their order can be permuted without loss of generality. Hence, we obtain Fig. 7b.

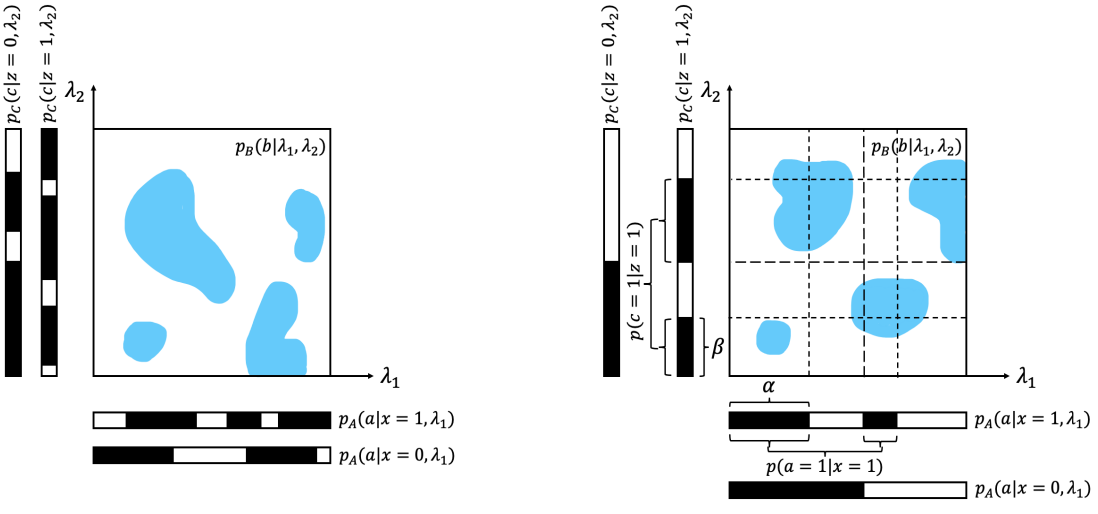

(a) Before ordering.

(b) After ordering

Figure 7: Representation of a bilocal correlation. The coloured part corresponds to $p(a, b = 1, c|x, z)$.

This way of visualising local strategies divides the square into 16 rectangles (R_J with $J = 1, 2, ..., 16$) each corresponding to one of the 16 possible deterministic strategies that

Alice and Charlie decide upon receiving λ_1 and λ_2 respectively. In each rectangle, there can be a coloured part (which we will call S_J) and an uncoloured part that represent the probability of Bob outputting 1 or 0, respectively:

$$S_J = p(b = 1 \ \wedge \ \{\lambda_1, \lambda_2\} \in R_J). \tag{12}$$

Moreover, there are two more variables that are unobservable, α and β, which correspond to another two degrees of freedom that can be visualized in the Fig. 7b. So, in order to fulfill the locality condition, the variables S_J must fulfill certain conditions.

First, since the variables S_J corresponds to probabilities, they all have to fulfill positivity and have to be less than one,

$$S_J \geq 0 \ \text{ for } \ J = 0, 1, ..., 16. \tag{13}$$

$$S_J \leq 1 \ \text{ for } \ J = 0, 1, ..., 16. \tag{14}$$

Secondly, the variables S_J have to be smaller than the rectangles they are contained in,

$$S_J \leq R_J \ \text{ for } \ J = 0, 1, ..., 16. \tag{15}$$

Eq. (15) makes Eq. (14) redundant. All these conditions can be translated in terms of probabilities:

$$\begin{aligned}
S_1 &\leq \alpha \cdot \beta \\
S_2 &\leq [p(a = 1, b, c|x = 0, z = 0) - \alpha] \cdot \beta \\
S_3 &\leq [p(a = 1, b, c|x = 1, z = 0) - \alpha] \cdot \beta \\
S_4 &\leq [p(a = 1, b, c|x = 1, z = 0) - p(a = 1, b, c|x = 0, z = 0) + \alpha] \cdot \beta \\
S_5 &\leq \alpha \cdot [p(a, b, c = 1|x = 0, z = 0) - \beta] \\
S_6 &\leq [p(a = 1, b, c|x = 0, z = 0) - \alpha] \cdot [p(a, b, c = 1|x = 0, z = 0) - \beta] \\
S_7 &\leq [p(a = 1, b, c|x = 1, z = 0) - \alpha] \cdot [p(a, b, c = 1|x = 0, z = 0) - \beta] \\
S_8 &\leq [p(a = 1, b, c|x = 1, z = 0) - p(a = 1, b, c|x = 0, z = 0) + \alpha] \cdot [p(a, b, c = 1|x = 0, z = 0) - \beta] \\
S_9 &\leq \alpha \cdot [p(a, b, c = 1|x = 0, z = 1) - \beta] \\
S_{10} &\leq [p(a = 1, b, c|x = 0, z = 0) - \alpha] \cdot [p(a, b, c = 1|x = 0, z = 1) - \beta] \\
S_{11} &\leq [p(a = 1, b, c|x = 1, z = 0) - \alpha] \cdot [p(a, b, c = 1|x = 0, z = 1) - \beta] \\
S_{12} &\leq [p(a = 1, b, c|x = 1, z = 0) - p(a = 1, b, c|x = 0, z = 0) + \alpha] \cdot [p(a, b, c = 1|x = 0, z = 1) - \beta] \\
S_{13} &\leq \alpha \cdot [p(a, b, c = 1|x = 0, z = 1) - p(a, b, c = 1|x = 0, z = 0) + \beta] \\
S_{14} &\leq [p(a = 1, b, c|x = 0, z = 0) - \alpha] \cdot [p(a, b, c = 1|x = 0, z = 1) - p(a, b, c = 1|x = 0, z = 0) + \beta] \\
S_{15} &\leq [p(a = 1, b, c|x = 1, z = 0) - \alpha] \cdot [p(a, b, c = 1|x = 0, z = 1) - p(a, b, c = 1|x = 0, z = 0) + \beta] \\
S_{16} &\leq [p(a = 1, b, c|x = 1, z = 0) - p(a = 1, b, c|x = 0, z = 0) + \alpha] \cdot \\
&\quad \cdot [p(a, b, c = 1|x = 0, z = 1) - p(a, b, c = 1|x = 0, z = 0) + \beta] \,.
\end{aligned} \tag{16}$$

Additionally, some conditions on the Bob's response function have to be fulfilled. It is sufficient to look at $p(a, b = 1, c|x, z)$ (the coloured part in Fig. 7), since $p(a, b = 0, c|x, z) = p(a|x)p(c|z) - p(a, b = 1, c|x, z)$. These conditions can be represented by the Fig. 19 of Appendix C and can be written as follows:

$$
\begin{aligned}
&S_1 + S_2 + S_5 + S_6 = p(a=1, b=1, c=1|x=0, z=0)\\
&S_3 + S_4 + S_7 + S_8 = p(a=0, b=1, c=1|x=0, z=0)\\
&S_9 + S_{10} + S_{13} + S_{14} = p(a=1, b=1, c=0|x=0, z=0)\\
&S_{11} + S_{12} + S_{15} + S_{16} = p(a=0, b=1, c=0|x=0, z=0)\\
&S_1 + S_3 + S_5 + S_7 = p(a=1, b=1, c=1|x=1, z=0)\\
&S_9 + S_{11} + S_{13} + S_{15} = p(a=1, b=1, c=0|x=1, z=0)\\
&S_1 + S_2 + S_9 + S_{10} = p(a=1, b=1, c=1|x=0, z=1)\\
&S_3 + S_4 + S_{11} + S_{12} = p(a=0, b=1, c=1|x=0, z=1)\\
&S_1 + S_3 + S_9 + S_{11} = p(a=1, b=1, c=1|x=1, z=1).
\end{aligned}
\tag{17}
$$

Finally, observing the pictorial representation (Fig. 7b) the last conditions are:

$$
\begin{aligned}
&\alpha \geq 0\\
&\alpha \leq p(a=1|x=1)\\
&\alpha \leq p(a=1|x=0)\\
&\alpha \geq p(a=1|x=1) - p(a=0|x=0)\\
&\beta \geq 0\\
&\beta \leq p(c=1|z=1)\\
&\beta \leq p(c=1|z=0)\\
&\beta \geq p(c=1|z=1) - p(c=0|z=0),
\end{aligned}
\tag{18}
$$

but the third, the fourth and the last two equations of (18) are redundant with the other constraints. Then, we have 18 variables and 45 constraints. Notice that there are some constraints that are bilinear (Eq. (16)), as some of them have the term $\alpha\beta$. Then, it is a bilinear problem.

This problem can also be approached from another formalism, that uses a decomposition onto deterministic correlations with weights $q_{\bar{\alpha}\bar{\beta}\bar{\gamma}}$ [BGP10]. That is, a determistic strategy by Alice is defined by the output α_x that she assigns to each possible input x. This means that each deterministic strategy can be represented by the string $\bar{\alpha} = \alpha_0, \alpha_1, ..., \alpha_N$, where N corresponds to the number of possible inputs of Alice. Her corresponding response function will be $P_{\bar{\alpha}}(a|x) = \delta_{a,\alpha_x}$. Analogously, if we do the same for Bob and Charlie by calling $\bar{\beta}$ and $\bar{\gamma}$ their respective strategies, Eq. (11) can be rewritten as follows:

$$
p(a, b, c|x, y, z) = \sum_{\bar{\alpha},\bar{\beta},\bar{\gamma}} q_{\bar{\alpha}\bar{\beta}\bar{\gamma}} P_{\bar{\alpha}}(a|x) P_{\bar{\beta}}(b|y) P_{\bar{\gamma}}(c|z) \tag{19}
$$

where $q_{\bar{\alpha}\bar{\beta}\bar{\gamma}} = \int\int_{\Lambda^{12}_{\bar{\alpha}\bar{\beta}\bar{\gamma}}} d\lambda_1 d\lambda_2$ with $\Lambda^{12}_{\bar{\alpha}\bar{\beta}\bar{\gamma}}$ the set of all pairs (λ_1, λ_2) that determine the $\bar{\alpha}\bar{\beta}\bar{\gamma}$-strategy. It follows that $\sum_{\bar{\alpha},\bar{\beta},\bar{\gamma}} q_{\bar{\alpha}\bar{\beta}\bar{\gamma}} = 1$. In this notation, a bilocal correlation satisfies:

$$
q_{\bar{\alpha}\bar{\gamma}} = q_{\bar{\alpha}} q_{\bar{\gamma}} \tag{20}
$$

So, an equivalent implementation to the previous one can be done in these terms. Now the variables would be $q_{\bar{\alpha}\bar{\beta}\bar{\gamma}}$ and the constraints would be $q_{\bar{\alpha}\bar{\beta}\bar{\gamma}} \geq 0$ and Eq. (19) and (20). This results in a bilinear program that can be solved with Gurobi [Gur22]. In this way,

we obtain completely equivalent results to those obtained with the previous formalism. Moreover, this new approach is interesting because it can be easily generalized to other possible cases in the bilocal scenario including, for instance, more than one input for Bob.

2.2 IMPLEMENTATION AND TESTS

There are two possibilities to address the problem set out in subsection 2.1. The first one is to linearize the problem by taking, for example, β as a given constant (it would be equivalent to do it with α) and solving the problem for the different possibilities of β. So, by this way, the program becomes an "infinite set" of linear programs. However, a fairly good approximation is to solve a finite number of linear programs, i.e., discretizing the interval to which β belongs, defined by Eq. (18). A linear program is one that optimises a linear function (objective function) given linear constraints. Our linear program is a feasibility problem and can be written as:

$$\begin{aligned} \max_{S_J,\alpha,\beta} \quad & 1 \\ \text{s.t.} \quad & (16), (17), (18). \end{aligned} \tag{21}$$

where we are optimizing a scalar function because in a feasibility problem, every solution is optimal.

The second possibility is to make use of a program that allows us to solve bilinear problems. In our case, we have used Gurobi [Gur22], but there are other equivalent programs such as BMIBNB [BMI22]. Gurobi is a solver that uses the Branch and Bound method. This method makes it possible to find the optimal solution, after exploring different solutions. It is based on two tools: branching and bounding. First, the problem is solved by adding a linear relaxation. From the solution obtained, the problem is branched by adding constraints to the model. In this way, the process is repeated, obtaining different solutions that form a tree. As the tree is branched, the bounding is performed, thus discarding possible branches that are of no interest. Finally, the solver tells you whether or not it has found a solution and if it has, it gives you the values of the variables corresponding to it.

Using both methods, we succeed in obtaining an oracle that allows us to determine wheter a correlation is bilocal or not.

Several tests are carried out to benchmark the oracle. Using the bilinear program, one of them is to obtain the visibility (V) for which a solution begins to exist, i.e., to quantify the nonbilocality of a correlation by its resistance to noise. This means finding the visibility for which the following probability becomes bilocal:

$$p(a,b,c|x,y,z) = V \cdot p_{nonbilocal} + (1-V) \cdot p_{uniform}, \tag{22}$$

where $p_{nonbilocal}$ corresponds to a nonbilocal correlation and $p_{uniform}$, to the uniform probability.

For this purpose, we use a scenario that produces nonbilocal correlations. It is the entanglement swapping scenario in the cases in which Bob has one input and two, three or four outputs. First, we compute the problem in which Bob has two outputs that is defined in section 3.2.1 and we find a visibility of $V = 0.707 \simeq 1/\sqrt{2}$, which is what we expected. Notice that in this case the $p_{uniform}$ will be biased because of the coarse grained in Bob measurements, which corresponds to have $p(a, b = 0, c|x, z) = 1/16$ and $p(a, b = 1, c|x, z) = 3/16$. Then, we compute the analogous problem for the case in which Bob has three and four outputs and we obtain $V = 0.666 \simeq 2/3$ and $V = 1/2$, respectively. These two last visibilities coincides with what is expected from Ref. [BRGP12]. Notice that

in these cases, the pictorial representation is equivalent to the one described in section 2.1 but adding one or two more colours, respectively (see appendix D).

Then, these tests are carried out with the linear program which certified that it obtains the same results as the bilinear program. In addition, a plot can be generated to show whether or not there is a bilocal solution (with yellow or purple, respectively) depending on the visibility and the given β to see how it behaves. For the case in which Bob has two outputs, Fig. 8a is obtained. We can see the abrupt cutoff at $V = 0.707$ from which there are no more bilocal correlations.

Similarly, an equivalent study can be carried out for the case in which Bob has three outputs obtaining the Fig. 8b. In that plot, we can see that the bilocal solutions end for $V = 0.66$. It is remarkable that this plot is completely different from the one obtained for the case of Bob with 2 outputs. For completeness, the study for the case in which Bob has 4 outputs is shown in the Fig. 8c.

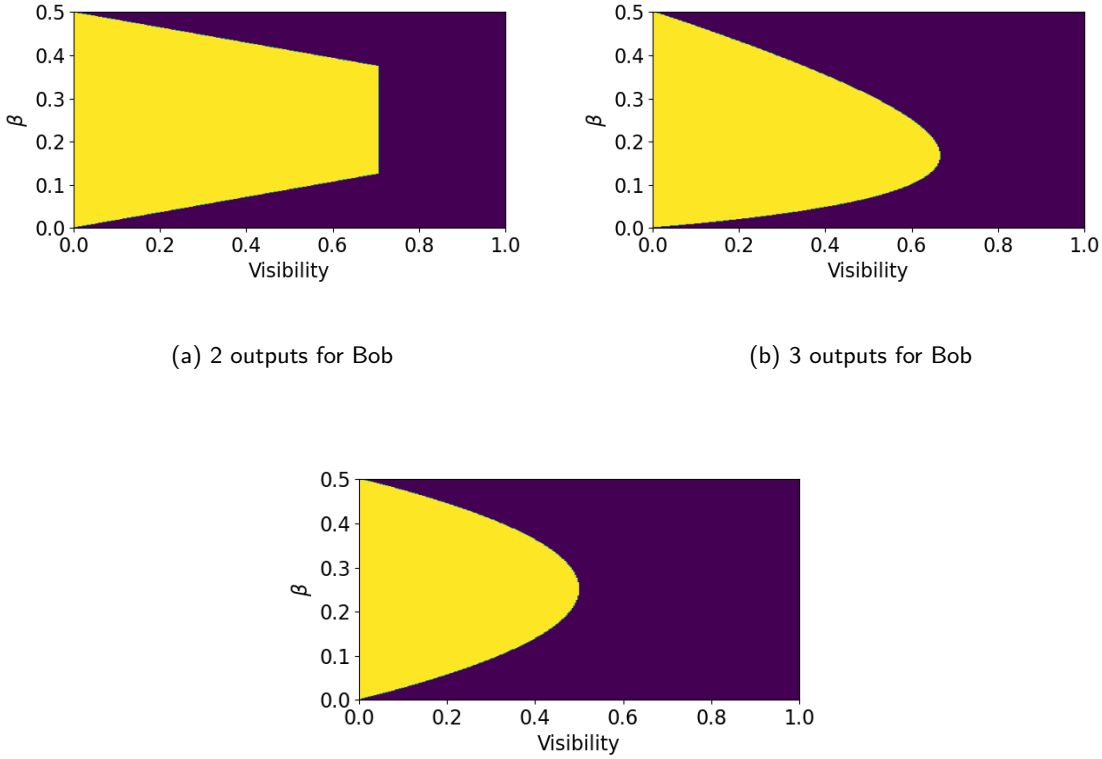

(a) 2 outputs for Bob

(b) 3 outputs for Bob

(c) 4 outputs for Bob

Figure 8: Representation of the solutions for the correlation given by Eq. (22) for each value of β and visibility in the entanglement-swapping scenario.

In order to test our program in a different scenario, we reproduce the results of the paper [TGB21] to compare our results with them. In that paper, they construct a plot equivalent to Fig. 8a for the Elegant Joint Measurement (EJM) in the bilocal scenario. This study does not go directly back to the standard quantum nonlocality as the ones based on Bell State Measurement. In an EJM (Fig. 9), Bob distributes different states to Alice and Charlie than in the Bell State Measurement case. To study the (non)bilocality

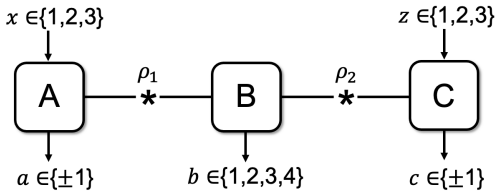

Figure 9: Representation of the scenario used for test the (non)bilocality with the Elegant Joint Measurement.

in that case, we use a bilocal scenario in which Alice and Charlie have three inputs and two outputs ($x, z \in \{1, 2, 3\}$ and $a, c \in \{\pm 1\}$) which corresponds to measurements of the three Pauli observables (σ_1, σ_2 and σ_3). Bob has one input and four outputs that corresponds to the result of the EJM ($b \in \{1, 2, 3, 4\}$), which is defined with more detail in Appendix E.

Furthermore, the two sources emit pair of qubits corresponding to the so-called Werner states:

$$\rho_i = V_i \left|\psi^-\right\rangle \left\langle\psi^-\right| + \frac{1 - V_i}{4}\mathbb{1}, \tag{23}$$

where $i \in \{0, 1\}$ and V_i is the visibility of each singlet. When Bob applies the EJM on pure singlets, an entangled state arises between Alice and Charlie. Moreover, the paper shows an analytical inequality:

$$\frac{S}{3} - T \overset{\text{biloc}}{\leq} 3 + 5Z, \tag{24}$$

where:

$$S = \sum_{y=z} \langle B^y C_z \rangle - \sum_{x=y} \langle A_x B^y \rangle, \quad T = \sum_{x \neq y \neq z \neq x} \langle A_x B^y C_z \rangle, \quad Z = \max\left(\mathcal{C}_{\text{other}}\right), \tag{25}$$

where $\mathcal{C}_{\text{other}} = \{|A_x|, |A_x B^y|, ..., |A_x B^y C_z|\}$ and all the correlators are given in Appendix E.

Implementing this scenario in our program, we can obtain a plot showing whether or not there is a solution as a function of V_1 and V_2 (Fig. 10). In this plot, we also show the analytical inequality they obtained. Moreover, the red dots corresponds to the results of [TGB21] observing that we obtain equivalent outcomes.

3 ANALYSIS OF THE BILOCAL SET

As the scope of this thesis is studying the simplest bilocality scenario defined in section 2, here we try to understand the shape of the set formed by the bilocal correlations of that scenario. Moreover, we are also interested in what is genuinely new with regard to the standard bipartite Bell scenario and in different ways of generating nonlocality.

3.1 UNDERSTANDING THE GEOMETRY OF THE SET

All the violations that have been discussed above for the "simplest" bilocal scenario (Fig. 6) correspond to quantum correlations that are nonlocal between Alice and Charlie (in the standard bipartite Bell scenario) when conditioning on Bob's output. Therefore it is natural to ask whether the following conjecture is true:

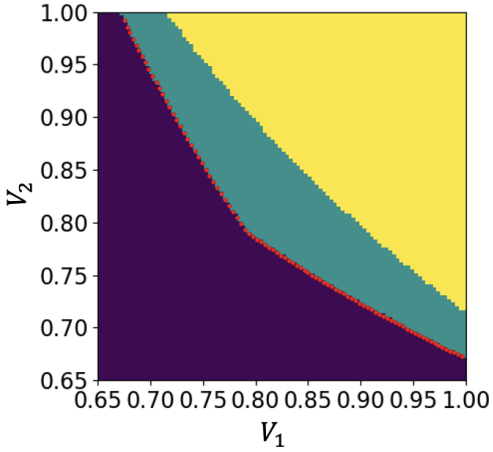

Figure 10: Representation of the feasibility for a bilocal solution for the scenario in Fig. 9. The purple area shows when there is no solution, the yellow area, when there is and such a solution can be obtained by means of the analytical inequality and the blue area, where there is solution but it cannot be obtained by the analytical inequality. Finally the red dots corresponds to the paper data [TGB21].

$$\left.\begin{aligned} p_0 \equiv \tfrac{p(a,b=0,c|x,z)}{p(b=0)} &\in \mathcal{L}^{Bell} \\ p_1 \equiv \tfrac{p(a,b=1,c|x,z)}{p(b=1)} &\in \mathcal{L}^{Bell} \\ p_A p_C \equiv p(a|x)p(c|z) &= w_0 p_0 + w_1 p_1 \end{aligned}\right\} \Leftrightarrow p(a,b,c|x,z) \in \mathcal{B}. \tag{26}$$

where $w_i = p(b=i)$ for $i = 0, 1$ and $w_0 + w_1 = 1$. We prove that the implication $\Leftarrow$ is true as follows.

Let us consider a bilocal distribution p. As it is bilocal, it can be written as equation 10. Hence, p_0 will be:

$$p_0 \equiv \frac{p(a,b=0,c|x,z)}{p(b=0)} = \frac{\int d\lambda_1 \int d\lambda_2 \mu(\lambda_1)\mu(\lambda_2) p(a|x\lambda_1) p(b=0|\lambda_1,\lambda_2) p(c|z,\lambda_2)}{\sum_{a,c} \int d\lambda_1 \int d\lambda_2 \mu(\lambda_1)\mu(\lambda_2) p(a|x\lambda_1) p(b=0|\lambda_1,\lambda_2) p(c|z,\lambda_2)}, \tag{27}$$

as $p(b=0) = \sum_{a,c} p(a,b=0,c|x,z)$. Using the fact that $\sum_a p(a,x|\lambda_1) = 1$ and, analogously, $\sum_c p(c|z,\lambda_2) = 1$, we get

$$p_0 = \frac{\int d\lambda_1 \int d\lambda_2 \mu(\lambda_1)\mu(\lambda_2) p(a|x\lambda_1) p(b=0|\lambda_1,\lambda_2) p(c|z,\lambda_2)}{\int d\lambda_1 \int d\lambda_2 \mu(\lambda_1)\mu(\lambda_2) p(b=0|\lambda_1,\lambda_2)}. \tag{28}$$

Moreover, we know that the set of bilocal correlations is inside the set composed by the local correlations of network with three parties. This can be easily seen as follows. A tripartite distribution is local if it can be written as

$$\int d\lambda \mu(\lambda) p(a|x\lambda) p(b|\lambda) p(c|z,\lambda). \tag{29}$$

Furthermore, any distribution of the form 10 is also of the form above, by choosing $\lambda = \{\lambda_1, \lambda_2\}$, $p(a|x\lambda) = p(a|x\lambda_1)$, $p(b|\lambda) = p(b|\lambda_1,\lambda_2)$ and $p(c|z,\lambda) = p(c|z,\lambda_2)$.

Then, if any bilocal correlation is also network local we can rewrite equation 28 as:

$$p_0 = \frac{\int d\lambda \mu(\lambda) p(a|x\lambda) p(b=0|\lambda) p(c|z,\lambda)}{\int d\lambda \mu(\lambda) p(b=0|\lambda)}. \tag{30}$$

In the numerator of this equation we can redefine the probability distribution $\mu(\lambda)$ absorbing $p(b=0|\lambda)$ and normalizing this probability distribution with the denominator, so

$$p_0 = \int d\lambda g_0(\lambda) p(a|x,\lambda) p(c|z,\lambda), \tag{31}$$

where $g_0(\lambda) = \frac{\mu(\lambda)p(b=0|\lambda)}{\int d\lambda \mu(\lambda)p(b=0|\lambda)}$. The form of the previous equation corresponds to the local decomposition (Eq. 1), so this complete the proof for the first condition of Eq. 26.

The second condition of equation 26 is completely analogous changing $b=0$ to $b=1$.

Finally, for the third condition of equation 26, we start from the definition of $p(a,c|x,z)$ and we only have to reorder the terms as follows:

$$\begin{aligned} p(a,c|x,z) = \sum_b p(a,b,c|x,z) = \sum_b \int d\lambda_1 \int d\lambda_2 \mu(\lambda_1)\mu(\lambda_2) p(a|x,\lambda_1) p(b|\lambda_1,\lambda_2) p(c|z,\lambda_2) = \\ = \int d\lambda_1 \mu(\lambda_1) p(a|x,\lambda_1) \int d\lambda_2 \mu(\lambda_2) p(c|z,\lambda_2) = p(a|x)p(c|z) \end{aligned} \tag{32}$$

Hence, the implication $\Leftarrow$ of the conjecture (Eq. 26) is proven. ■

However, we find later the conjecture to be false because of the implication $\Rightarrow$, it is:

$$\begin{gathered} \mathcal{B} \subsetneq \mathcal{B}' \\ \mathcal{B}' := \{p(abc|xz) \text{ such that } p(ac|xz) = p(a|x)p(c|z) \ \wedge \ p(ac|xz, b=i) \in \mathcal{L}\} \end{gathered} \tag{33}$$

and we prove the following lemmas to understand the shape of $\mathcal{B}$ inside $\mathcal{B}'$ and how they do not coincide.

Lemma 3.1. *Given a convex combination of p_0 and p_1 which results in $p_A p_C$, such that the resulting $p(abc|xz)$ is bilocally feasible:*

$$p_A p_C = w_0 p_0 + w_1 p_1, \tag{34}$$

we can always reproduce bilocally any combination between two points that lie, one on the segment joining p_0 and $p_A p_C$ (p_0') and the other on the segment joining p_1 and $p_A p_C$ (p_1') (see Fig. 21 in Appendix F), which also results in $p_A p_C$:

$$p_A p_C = w_0' p_0' + w_1' p_1', \tag{35}$$

where $w_i' = p'(b=i)$ for $i=0,1$ and, naturally, $w_0' + w_1' = 1$. See proof in Appendix F.

Lemma 3.2. *Given two bilocal distributions $p'(a,b,c|x,z)$ and $p''(a,b,c|x,z)$ that factorizes in $p_A p_C$, we can always construct a probability $p(a,b,c|x,z)$ that also factorizes in $p_A p_C$ making a convex combinations between p', p'' and $p_A p_C$.*

$$p_A p_C = w_0 p_0 + w_1 p_1. \tag{36}$$

See proof in Appendix G.

Intuitively, this last lemma allows us to explore the points that join p_0' and p_0'' and p_1' and p_1'' pictorially represented in Fig. 11. Hence, mixing these two previous lemmas we are able to explore the blue region of Fig. 11. We also studied the optimal choice to obtain the largest posible blue region.

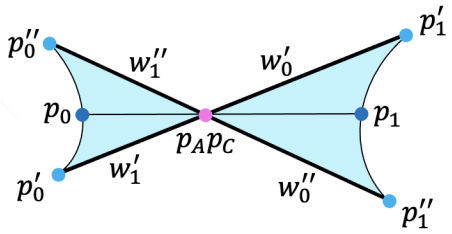

Figure 11: Representation of the different possibilities of convex combinations between $p'(a,b,c|x,z)$ and $p''(a,b,c|x,z)$ which result in $p_A p_C$.

Lemma 3.3. *Given a convex combination between p_0 and p_1 which results in $p_A p_C$, $w_0 p_0 + w_1 p_1 = p_A p_C$ with $w_0 + w_1 = 1$ is satisfied. Therefore, if $p_A p_C$, p_1 and w_1 are given, all the rest is fixed. The lemma states that we can choose p_1 to be any local distribution as far as $w_1 = \varepsilon$ is small enough (see Fig. 23 in Appendix H).*

See proof in Appendix H.

3.1.1 Disproving the conjecture

We can use the last lemma to try to find a counterexample. If we look for the maximum ε for a probability distribution to be bilocal two things can happen: that the ε for which $p(a,b,c|x,z)$ ceases to be bilocal coincides with the one for which p_0 ceases to be local (in this case the conjecture could be true) or that the ε for which p_0 ceases to be local is greater than the one for which $p(a,b,c|x,z)$ ceases to be bilocal (we would have a counterexample). Indeed, making use of this, several counterexamples can be found. Notice that, although with that counterexamples we know that the previous conjecture is not true, it might still be true if p is constrained to be feasible in quantum bilocality.

Numerically, exploring each of the 16 vertices of the local polytope (corresponding to the 16 deterministic strategies) in this way, no counterexamples are found, but if we define p_1 as the convex combination of two of these vertices,

$$p_1 = \mu p_1' + (1-\mu) p_1'', \tag{37}$$

we find counterexamples. One counterexample is found for the case in which p_1 corresponds to the convex combination between the following deterministic strategies:

x'	z'	a'	c'	x''	z''	a''	c''
0	0	1	1	0	0	0	0
0	1	1	1	0	1	0	1
1	0	1	1	1	0	1	0
1	1	1	1	1	1	1	1

This can be seen in Fig. 12, as the plots show a gap between the maximum ε for which p_1 is local and the maximum ε for which $p(a,b,c|x,z)$ is bilocal.

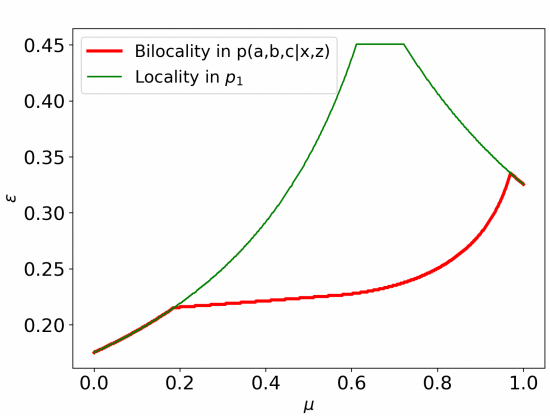

Figure 12: Comparation between the maximum ε for which p_1 is local and the one for which $p(a,b,c|x,z)$ is bilocal in function of μ.

We can see if what we are obtaining numerically for the bilocal prediction corresponds to what is expected. For this purpose, imagine that p_1 corresponds to the following deterministic strategy:

x	z		a	c
0	0		1	1
0	1	→	1	0
1	0		1	1
1	1		1	0

This strategy refers to the coloured square of Fig. 13a. The maximum ε for which $p(a,b,c|x,z)$ is still bilocal corresponds to the maximum area that the square (corresponding to the deterministic strategy) can take as a function of α and β. Hence, the maximum ε will be:

$$\max\{\varepsilon\} = \max_{\alpha,\beta}\{\alpha(p(c=1|z=0)-\beta)\}, \tag{38}$$

such that α and β fulfill their corresponding bounds:

$$\begin{aligned}\max\{0, p(a=1|x=1)-p(a=0|x=0)\} \leq \alpha \leq \min\{p(a=1|x=1), p(a=1|x=0)\}\\ \max\{0, p(c=1|z=1)-p(c=0|z=0)\} \leq \beta \leq \min\{p(c=1|z=1), p(c=1|z=0)\}\end{aligned} \tag{39}$$

The ε obtained with the numerical simulation and with the above formula coincides for any given $p_A p_C$.

In the case where p_1 is defined as the convex combination between two deterministic strategies (Eq. (37)), the maximum ε corresponds to the sum of the maximum possible coloured area in the two squares corresponding to these deterministic strategies. If we study the case that gives us a counterexample above, this is to have one of the squares completely coloured and the other partially coloured (Fig. 13b). For this specific case, the maximum epsilon is:

$$\max\{\varepsilon\} = \frac{1}{\mu}\max_{\alpha,\beta}\left\{\min\left[\alpha\beta, \frac{\mu}{1-\mu}(p(a=1|x=1)-\alpha)(p(c=1|z=1)-\beta)\right]\right\}. \tag{40}$$

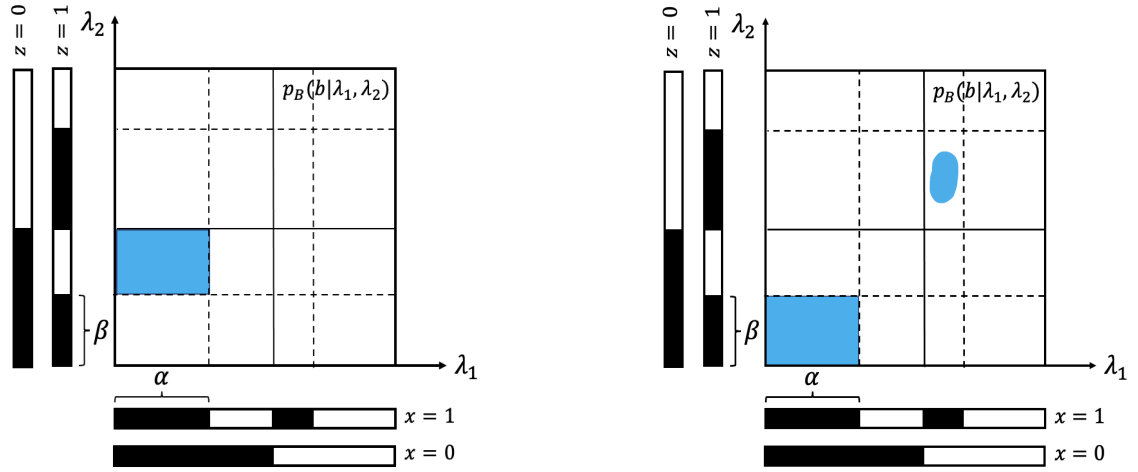

(a) Before ordering.

(b) After ordering

Figure 13: Representation of a bilocal correlation. The coloured part in the square corresponds to $p(a, b = 1, c|x, z)$. The coloured part in the bars corresponds to output $a = 1$ for the horizontal ones and $c = 1$ in the vertical ones.

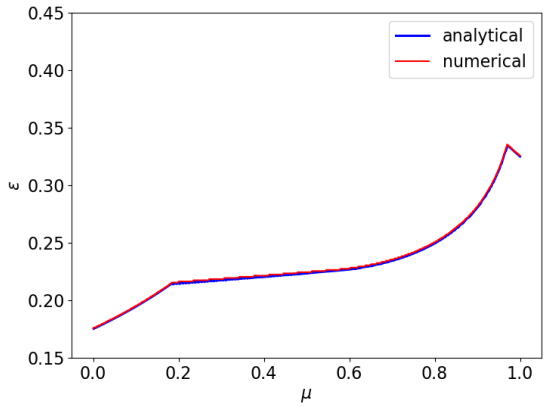

Figure 14: Comparation between the numerical and the analytical prediction for the maximum ε for which for which $p(a, b, c|x, z)$ is bilocal in function of μ.

That equation also reproduces what we obtain numerically (Fig. 14).

Notice that this can be generalize for a convex combination of any number of deterministic strategies.

3.2 GENUINE NONLOCALITY

In order to understand better the bilocal set, we study two different ways of producing nonbilocality (we call them "cheating scenarios") that are based on standard Bell nonlocality and, therefore, might be seen as nongenuine. It is hard to define what is or not genuine. We understand that a scenario is genuinely nonlocal when you cannot trace back to the standard Bell scenario, but some authors have different definitions (see [ŠBCB22]). Then, we mix these cheating scenarios and we find genuine nonbilocality. The overall picture shows that not only the geometry of the bilocal set is complex, but also that genuine nonbilocality that can be achieved with quantum sources is highly nontrivial.

3.2.1 Entanglement-swapping

Entanglement-swapping is one of the most popular phenomena that produces nonlocality in the bilocal scenario. It consists in making two particles that have never interacted to be nonlocally correlated. Let us consider a scenario as the one depicted in Fig. 6. In it, both sources emit a maximally entangled state, say $|\phi^+\rangle$. Bob makes a coarse grained Bell basis measurement on the shares he receives from the sources. That is, given the four maximally entangled states $|\psi^+\rangle, |\psi^-\rangle, |\phi^+\rangle, |\phi^-\rangle$, he makes a projective measurement that outputs 0 when the result is $|\psi^+\rangle$, while outputs 1 elsewhere. Then, his two measurement operators are $\hat{B}_0 = |\psi^+\rangle\langle\psi^+|$ and $\hat{B}_1 = \mathbb{1} - |\psi^+\rangle\langle\psi^+|$. This means that when Bob outputs 0, he performed entanglement swapping, and Alice and Charlie will be sharing a maximally entangled state. On the other hand, Alice and Charlie perform the measurements such that when Bob outputs 0, they can violate the CHSH inequality. Concretely, they can perform measurements that maximally violate the CHSH inequality, it is $\hat{A}_0 = (\sigma_x - \sigma_z)/\sqrt{2}$, $\hat{A}_1 = (\sigma_x + \sigma_z)/\sqrt{2}$, $\hat{C}_0 = \sigma_x$ and $\hat{C}_1 = \sigma_z$. In this sense, we are violating bilocality by violating locality (according to Eq. (33) and Appendix A).

3.2.2 Fritz argument

There exists another way to generate nonlocality considered by T. Fritz in [Fri12] (Fig. 15). In that case, Bob and Charlie share a source λ that can give 0 or 1. Bob's measurement is determined by λ and Charlie directly outputs that λ and ignores z. So, it can be interpreted as an scenario in which Charlie's output becomes Bob's input. Moreover, in this scenario conditioning on Charlie, Alice and Bob violates the CHSH inequality. Thus, we can construct the following correlation:

$$p(a,b|x,c,z) = \frac{p(a,b,c|x,z)}{p(c|z)} \equiv p_z(a,b|x,c). \tag{41}$$

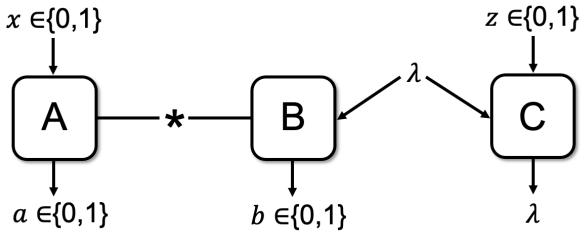

Figure 15: Representation of the cheating scenario without entanglement swapping.

We can test the CHSH in the previous correlation:

$$\begin{aligned} -2 \leq S_{CHSH} &= \sum_{a,b}(-1)^{a+b}\left(p_z(a,b|0,0) + p_z(a,b|0,1) + p_z(a,b|1,0) - p_z(a,b|1,1)\right) \leq 2 \Rightarrow \\ -2 \leq \sum_{a,b}(-1)^{a+b} &\left(\frac{p(a,b,0|0,z)}{p(c=0|z)} + \frac{p(a,b,1|0,z)}{p(c=1|z)} + \frac{p(a,b,0|1,z)}{p(c=0|z)} - \frac{p(a,b,1|1,z)}{p(c=1|z)}\right) \leq 2. \end{aligned} \tag{42}$$

Notice that this inequality is nonlinear in p. We can check if this inequality is satisfied by all bilocal scenarios or not. Furthermore, we can study in our previous counterexamples if there is a gap between the previous considered condition (the locality of p_0 and p_1) and this inequality. Looking for the maximum ε for which Eq. (42) is satisfied, it is found that all

bilocal correlations fulfil this inequality, as already known, but there are certain correlations that fulfil this inequality without being bilocal, so again it would be a necessary but not sufficient condition. Moreover, it is observed that there is a gap between the condition discussed in the previous section and this inequality, so there are correlations that violate one without violating the other and vice versa (Fig. 16).

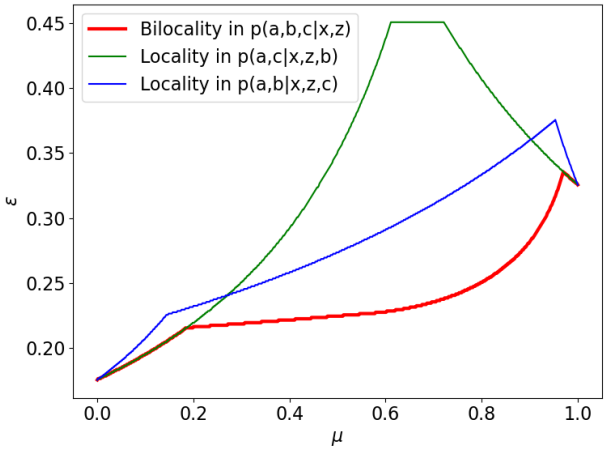

Figure 16: Representation of the dependence of ε with μ. The green line represents the maximum ε for which p_1 is local, the blue one, the maximum ε for which Eq. (42) is fulfilled and the red one, the maximum ε for which $p(a,b,c|x,z)$ is bilocal.

3.2.3 Mixing cheating scenarios

In the previous sections, we have found necessary conditions and some examples that fulfill that conditions being nonbilocal. However, it is not known wether these examples are quantumly feasible or not. What is known to be quantumly feasible are the entanglement-swapping scenario, described in the subsection 3.2.1, and the one depicted by Fig. 15. Moreover, another way to get information is to know which one of the previous conditions are fulfilled if we do a convex combination between these two scenarios. Despite of the fact that the quantum bilocal set is nonconvex and, therefore, a convex combination of two correlation can be quantumly nonbilocal, this mixing can be made because it relies in a convex combination between two of the three parties.

For this purpose, let us define:

$$p(a,b,c|x,z) = \mu \cdot p_{ent} + (1-\mu) \cdot p_{Fritz}, \tag{43}$$

where p_{ent} corresponds to the correlation of the entanglement swapping scenario and p_{Fritz}, to the correlation of the one of Fig. 15. In Fig. 17, it is shown for which μ these conditions are or not satisfied. Those conditions are: bilocality of $p(a,b,c|x,z)$, locality of $p(a,c|x,z,b)$ (where b becomes a parameter), and locality of $p(a,b|x,c,z)$ (where z becomes a parameter).

These plots show us that there are examples that can be done quantumly in which without being bilocal, the conditions can be satisfied, either separately or both at the same time.

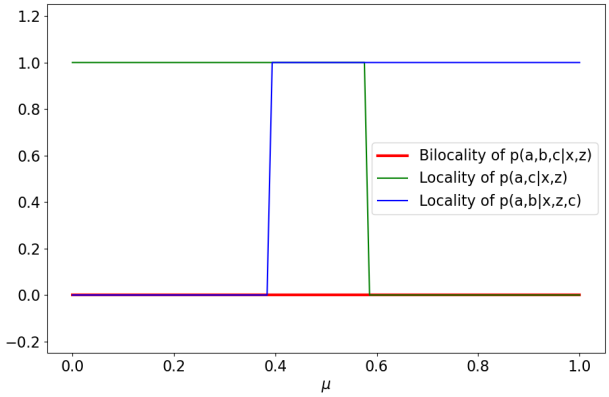

Figure 17: Representation of the bilocality, the locality condition and the Fritz condition in function of μ. One means that the condition is satisfied and zero, that is not.

4 CONCLUSION

The concept of nonlocality, which arises from the Bell Theorem and the standard Bell scenario and extends to more complex network scenarios, has been studied. The study of network nonlocality becomes challenging by the fact that the correlations originating from it form a non-convex set. In particular, this thesis focuses on the problem of characterising the simplest non-trivial bilocal network, whose complete characterization remains an open problem.

The first objective was to compute an oracle that tells us whether a correlation is bilocal or not. This was done by two methods with which we achieved equivalent results: solving a bilinear problem using the Gurobi solver and linearizing the problem and dealing with it by solving an array of the linear programs. Moreover, an alternative formalism to pose the problem was studied and thanks to that formalism, the oracle can be generalized to any bilocal scenario. Both methods and formalisms were checked by carrying out several tests.

After getting this tool to explore the bilocal set, we tried to analysed the geometry of that set. Observing the tests, we conjectured that a correlation is bilocal if and only if it factorizes when marginalising on Alice-Charlie and it is Bell-local when conditioning on Bob's output. We stated and proved different lemmas that helped us finding counterexamples to such conjecture and explore the geometry of the bilocal set. In general, even in such simple scenario we saw that the bilocal set is nontrivial.

Finally, we asked ourselves what is genuinely new in nonlocality related to the standard bipartite Bell scenario. We studied two scenarios that generate nonbilocality using quantum sources, relying on hidden violations of the standard bipartite CHSH inequality. Both of them can be seen as nongenuine, as their nonbilocality can be traced back to the standard Bell scenario. But, what is really surprising is that when we mixed these two scenarios, we find nonbilocality that cannot be traced back to either of the two, showing that the concept of genuine nonlocality is nontrivial at all.

The problem of the characterization of the bilocal set of correlations is still open, even if we have achieved an approach from inside. Currently, we are exploring different methods to get analytical inequalities. Furthermore, the tools obtained in this work can be used to explore more complicated bilocal scenarios (by adding inputs and/or outputs) or even different scenarios, such as the star network scenarios.

References

[AGR81] Alain Aspect, Philippe Grangier, and Gérard Roger. Experimental tests of realistic local theories via bell's theorem. *Physical review letters*, 47(7):460, 1981.

[BCP+14] Nicolas Brunner, Daniel Cavalcanti, Stefano Pironio, Valerio Scarani, and Stephanie Wehner. Bell nonlocality. *Reviews of Modern Physics*, 86(2):419, 2014.

[Bel64] John S Bell. On the einstein podolsky rosen paradox. *Physics Physique Fizika*, 1(3):195, 1964.

[BGP10] Cyril Branciard, Nicolas Gisin, and Stefano Pironio. Characterizing the nonlocal correlations created via entanglement swapping. *Physical review letters*, 104(17):170401, 2010.

[BMI22] BMIBNB Optimization. BMIBNB Optimizer Reference Manual, 2022.

[BRGP12] Cyril Branciard, Denis Rosset, Nicolas Gisin, and Stefano Pironio. Bilocal versus nonbilocal correlations in entanglement-swapping experiments. *Physical Review A*, 85(3):032119, 2012.

[CHSH69] John F Clauser, Michael A Horne, Abner Shimony, and Richard A Holt. Proposed experiment to test local hidden-variable theories. *Physical review letters*, 23(15):880, 1969.

[Cir80] Boris S Cirel'son. Quantum generalizations of bell's inequality. *Letters in Mathematical Physics*, 4(2):93–100, 1980.

[EPR35] A. Einstein, B. Podolsky, and N. Rosen. Can quantum-mechanical description of physical reality be considered complete? *Phys. Rev.*, 47:777–780, May 1935.

[FC72] Stuart J Freedman and John F Clauser. Experimental test of local hidden-variable theories. *Physical Review Letters*, 28(14):938, 1972.

[Fri12] Tobias Fritz. Beyond bell's theorem: correlation scenarios. *New Journal of Physics*, 14(10):103001, 2012.

[Gur22] Gurobi Optimization, LLC. Gurobi Optimizer Reference Manual, 2022.

[ŠBCB22] Ivan Šupić, Jean-Daniel Bancal, Yu Cai, and Nicolas Brunner. Genuine network quantum nonlocality and self-testing. *Physical Review A*, 105(2):022206, 2022.

[TBZG98] Wolfgang Tittel, Jürgen Brendel, Hugo Zbinden, and Nicolas Gisin. Violation of bell inequalities by photons more than 10 km apart. *Physical review letters*, 81(17):3563, 1998.

[TGB21] Armin Tavakoli, Nicolas Gisin, and Cyril Branciard. Bilocal bell inequalities violated by the quantum elegant joint measurement. *Physical review letters*, 126(22):220401, 2021.

[TPKR+21] Armin Tavakoli, Alejandro Pozas-Kerstjens, Marc-Olivier Renou, et al. Bell nonlocality in networks. *Reports on Progress in Physics*, 2021.

A Proof of the CHSH inequality

We will prove the CHSH inequality (Eq. 3) which is fulfilled if the correlation is local. Let us consider the standard Bell scenario with binary inputs and outputs (Fig. 18), where λ denotes a classical source of randomness. Without loss of generality λ can be a uniform random number between 0 and 1.

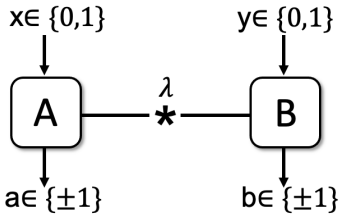

Figure 18: Representation of the standard Bell scenario with binary inputs and outputs

Moreover, without loss of generality the response functions are deterministic functions of λ. $A_x(\lambda) = \pm 1$ denotes the output of the party A given λ and an input x and, analogously, for the party B, $B_y(\lambda) = \pm 1$. Let us define the correlators:

$$\langle A_x B_y \rangle_\lambda = \int_0^1 d\lambda A_x(\lambda) B_y(\lambda). \tag{44}$$

The CHSH inequality with this definition can be rewritten as:

$$|S_{CHSH}| = \left| \int_0^1 d\lambda A_0(\lambda)B_0(\lambda) + \int_0^1 d\lambda A_0(\lambda)B_1(\lambda) + \int_0^1 d\lambda A_1(\lambda)B_0(\lambda) - \int_0^1 d\lambda A_1(\lambda)B_1(\lambda) \right|. \tag{45}$$

Defining $A_+(\lambda) \equiv A_0(\lambda) + A_1(\lambda)$ and $A_-(\lambda) = A_0(\lambda) - A_1(\lambda)$, the previous equation becomes:

$$|S_{CHSH}| = \left| \int_0^1 d\lambda A_+(\lambda)B_0(\lambda) + A_-(\lambda)B_1(\lambda) \right|, \tag{46}$$

and using the triangular inequality:

$$|S_{CHSH}| \leq \int_0^1 d\lambda |A_+(\lambda)B_0(\lambda)| + |A_-(\lambda)B_1(\lambda)| = \int_0^1 d\lambda |A_+(\lambda)||B_0(\lambda)| + |A_-(\lambda)||B_1(\lambda)| \tag{47}$$

It is known that $|A_x(\lambda)| = 1$ for $x = 0, 1$ and $|B_y(\lambda)| = 1$ for $y = 0, 1$. This implies that $A_+(\lambda)$ and $A_-(\lambda)$ can take the values 0,2 and -2 and if the former is ± 2, the latter is 0 and viceversa. Then, $|A_+(\lambda)| + |A_-(\lambda)| = 2$. Hence, taking into account all these statements, we get to the CHSH inequality:

$$|S_{CHSH}| \leq 2 \Rightarrow -2 \leq S_{CHSH} \leq 2 \qquad \blacksquare. \tag{48}$$

B Maximal violation of the CHSH

We will prove here the maximal violation of the CHSH inequality inside the quantum set. Let us rewrite the inequality with a slightly different notation:

$$\langle \psi | \, A_0 \otimes B_0 + A_0 \otimes B_1 + A_1 \otimes B_0 - A_1 \otimes B_1 \, | \psi \rangle \leq 2\sqrt{2}, \tag{49}$$

where $|\psi\rangle$ is a generic quantum state and $A_0, A_1, B_0, B_1 \in \mathbb{C}^d \otimes \mathbb{C}^d$ for any dimension d. Let us now define the following equation:

$$\left(\mathbb{1} - A_0 \otimes \frac{B_0 + B_1}{\sqrt{2}}\right)\left(\mathbb{1} - A_0 \otimes \frac{B_0 + B_1}{\sqrt{2}}\right) + \left(\mathbb{1} - A_1 \otimes \frac{B_0 - B_1}{\sqrt{2}}\right)\left(\mathbb{1} - A_1 \otimes \frac{B_0 - B_1}{\sqrt{2}}\right) \geq 0, \tag{50}$$

which is satisfied because it has the form $C_1^2 + C_2^2$ and this is by definition positive semidefinite. Manipulating that equation and using the fact that $A_0^2 = A_1^2 = B_0^2 = B_1^2 = \mathbb{1}$, we finally arrives to:

$$A_0 \otimes B_0 + A_0 \otimes B_1 + A_1 \otimes B_0 - A_1 \otimes B_1 \leq 2\sqrt{2}. \tag{51}$$

Hence, this proves that the maximal violation of the CHSH inequality inside the local set is $2\sqrt{2}$.

C Pictorial representation of the conditions on Bob's outputs

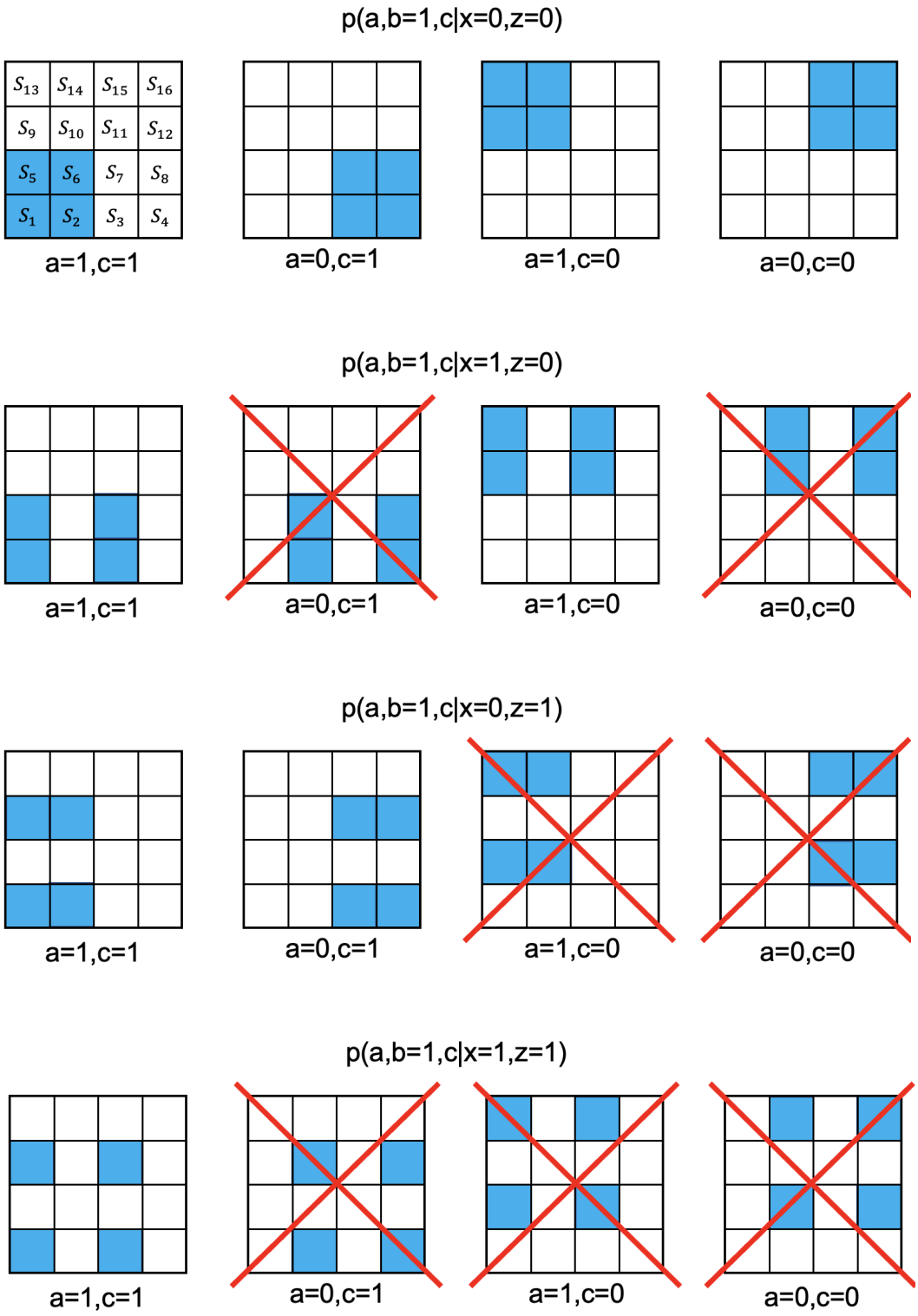

Figure 19: Representation of the conditions in Bob's response function. The red crosses indicate the redundant conditions.

D Pictorial representation when Bob has 3 outputs

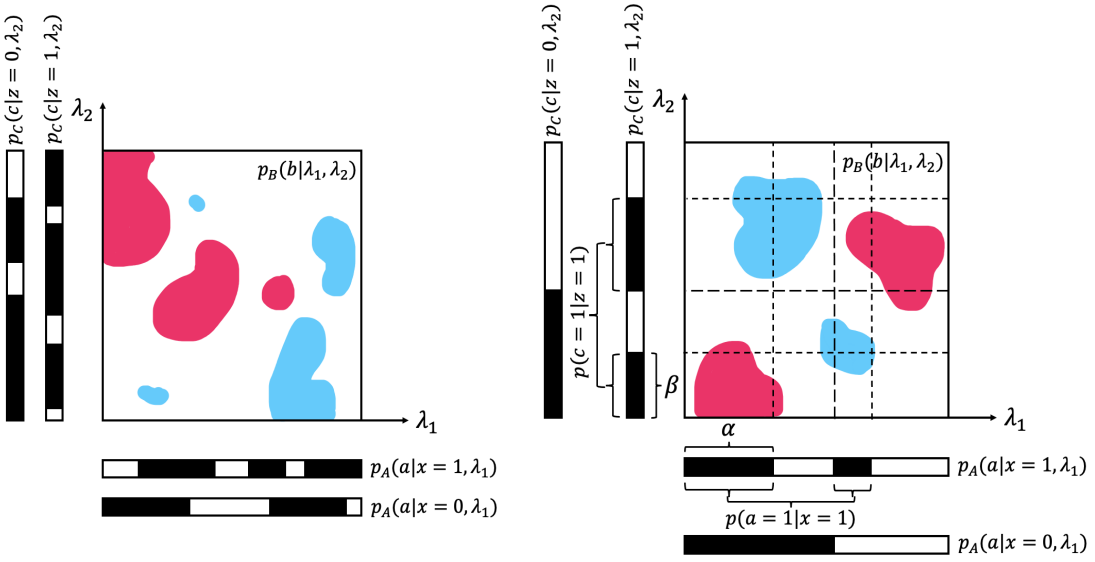

(a) Before ordering. (b) After ordering

Figure 20: Representation of a local correlation for the bilocal scenario when Bob has 1 input and 3 outputs. The blue area part corresponds to $p(a, b = 1, c|x, z)$.

E Elegant Joint Measurment

To apply the EJM, Bob applies the projectors $B_b = \left|\phi_b^\theta\right\rangle\left\langle\phi_b^\theta\right|$ with $b = 1, 2, 3, 4$ and $\theta \in [0, \pi/2]$ and where $\left|\phi_b^\theta\right\rangle$ is defined as follows:

$$\left|\Phi_b^\theta\right\rangle = \frac{\sqrt{3}+e^{i\theta}}{2\sqrt{2}}\left|\vec{m}_b, -\vec{m}_b\right\rangle + \frac{\sqrt{3}-e^{i\theta}}{2\sqrt{2}}\left|-\vec{m}_b, \vec{m}_b\right\rangle. \tag{52}$$

$$|\pm\vec{m}_b\rangle = \sqrt{\frac{1\pm\eta_b}{2}}e^{-i\varphi_b/2}|0\rangle \pm \sqrt{\frac{1\mp\eta_b}{2}}e^{i\varphi_b/2}|1\rangle. \tag{53}$$

$$\vec{m}_b = \sqrt{3}\left(\sqrt{1-\eta_b^2}\cos\varphi_b, \sqrt{1-\eta_b^2}\sin\varphi_b, \eta_b\right). \tag{54}$$

For our specific case, we have:

$$\begin{array}{ll} \vec{m}_1 = (+1,+1,+1), & \vec{m}_2 = (+1,-1,-1), \\ \vec{m}_3 = (-1,+1,-1), & \vec{m}_4 = (-1,-1,+1) \end{array}. \tag{55}$$

On the other side, the correlators used in the inequality take the following values:

$$\begin{aligned} &\langle A_x\rangle = \langle B^y\rangle = \langle C_z\rangle = \langle A_x C_z\rangle = 0 \\ &\langle A_x B^y\rangle = -\frac{V_1}{2}\cos\theta\delta_{x,y}, \quad \langle B^y C_z\rangle = \frac{V_2}{2}\cos\theta\delta_{y,z} \\ &\langle A_x B^y C_z\rangle = \begin{cases} -\frac{V_1V_2}{2}(1+\sin\theta) & \text{if } xyz \in \{123, 231, 312\} \\ -\frac{V_1V_2}{2}(1-\sin\theta) & \text{if } xyz \in \{132, 213, 321\} \\ 0 & \text{otherwise} \end{cases}. \end{aligned} \tag{56}$$

F Proof lemma 3.1

To prove this lemma, we assume that we have a distribution p which is bilocal (it satisfies the conditions of the left-hand side of the equation 26) and can, therefore, be written as equation 11.

Moreover, Bob chooses to follow this distribution p with probability α and with probability $(1-\alpha)$, he behaves following another strategy $\tilde{p}(b)$, that is independent on λ_1 and λ_2. Thus constructing a new probability distribution p' which also gives $p_A p_C$ when we marginalize in Bob:

$$p'(a,b,c|x,z) = \int_0^1 \int_0^1 d\lambda_1 d\lambda_2 p_A(a|x\lambda_1) \begin{pmatrix} \alpha\, p_B(b|\lambda_1\lambda_2) \\ + \\ (1-\alpha)\,\tilde{p}(b) \end{pmatrix} p_C(c|z\lambda_2). \tag{57}$$

Hence, p'_0 is determined by a convex combination between p_0 and $p_A p_C$ (Eq. 58) and, analogously, p'_1, between p_1 and $p_A p_C$ (Eq. 59). Intuitively, the points p'_0 and p'_1 will lie in the segment between p_0 and p_1 and will be determined by two degrees of freedom, α and $\tilde{p}(b)$ (see Fig. 21).

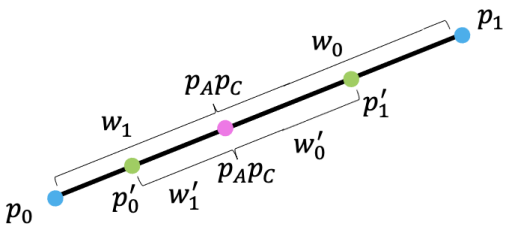

Figure 21: Representation of the different possibilities of convex combinations which result in $p_A p_C$, where all the points belong to $\mathcal{L}$.

$$p'_0 = \gamma_a p_0 + \gamma'_a p_A p_C$$
$$\text{with} \quad \gamma_a = \frac{\alpha p(b=0)}{\alpha p(b=0) + (1-\alpha)\tilde{p}(b=0)} \quad \text{and} \quad \gamma'_a = \frac{(1-\alpha)\tilde{p}(b=0)}{\alpha p(b=0) + (1-\alpha)\tilde{p}(b=0)} \tag{58}$$

$$p'_1 = \gamma_b p_1 + \gamma'_b p_A p_C$$
$$\text{with} \quad \gamma_b = \frac{\alpha p(b=1)}{\alpha p(b=1) + (1-\alpha)\tilde{p}(b=1)} \quad \text{and} \quad \gamma'_b = \frac{(1-\alpha)\tilde{p}(b=1)}{\alpha p(b=1) + (1-\alpha)\tilde{p}(b=1)}, \tag{59}$$

where naturally $\gamma_i + \gamma'_i = 1$ with $i = a, b$.
A convex combination of these p'_0 and p'_1 give us $p_A p_C$, as the lemma states (Eq. 35) with the following weights:

$$w'_i = \alpha p_B(b=i|\lambda_1,\lambda_2) + (1-\alpha)\tilde{p}(b=i) \quad \text{for } i = 0, 1. \tag{60}$$

■

G Proof lemma 3.2

Proof: due to the fact that $p'(a,b,c|x,z)$ and $p''(a,b,c|x,z)$ are bilocal distributions, they can be written as equation 11. Furthermore, we can assume that there is a coin that with

probability μ decides that λ_1 follows the first strategy ($p'(a,b,c|x,z)$) and with probability $(1-\mu)$, the second ($p''(a,b,c|x,z)$) and, similarly another coin, decides with probability ν and $(1-\nu)$ whether λ_2 follows the first or the second strategy, respectively (Fig. 22). We can impose that when both sources indicate the same strategy, the correlation will follow the indicated distribution, while when they indicate different ones, Bob will behave according to $\tilde{p}(b)$, which is independent of λ_1 and λ_2.

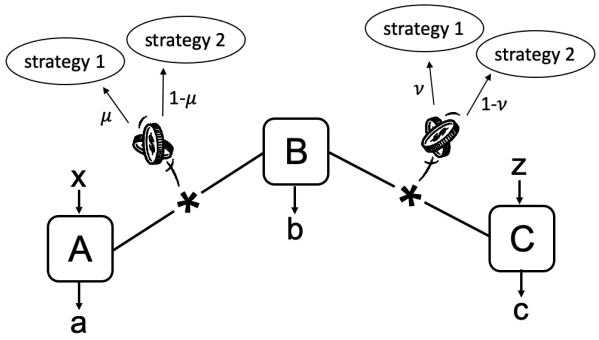

Figure 22: Representation of the behaviour of the sources.

Analogous to the proof of the previous lemma, p_0 is given by the convex combination of p'_0, p''_0 and $p_A p_C$:

$$p_0 = \gamma'_0 p'_0 + \gamma''_0 p''_0 + \tilde{\gamma}_0 p_A p_C, \tag{61}$$

where

$$\gamma'_0 = \frac{\mu\nu p'(b=0)}{\mu\nu p'(b=0) + (1-\mu)(1-\nu)p''(b=0) + (\mu+\nu-2\mu\nu)\tilde{p}(b=0)},$$
$$\gamma''_0 = \frac{(1-\mu)(1-\nu)p''(b=0)}{\mu\nu p'(b=0) + (1-\mu)(1-\nu)p''(b=0) + (\mu+\nu-2\mu\nu)\tilde{p}(b=0)},$$
$$\tilde{\gamma}_0 = \frac{(\mu+\nu-2\mu\nu)\tilde{p}(b=0)}{\mu\nu p'(b=0) + (1-\mu)(1-\nu)p''(b=0) + (\mu+\nu-2\mu\nu)\tilde{p}(b=0)}$$

and analogue expressions for p_1. Thus finding the p_0 and p_1 whose convex combination gives us $p_A p_C$.

■

H Proof of lemma 3.3

Proof: We prove this lemma by taking p_1 as one of the 16 possible deterministic strategies (corresponding to one of the 16 vertices of the local polytope) and p_0 as a point ε-close to $p_A p_C$. As a consequence we can always push p_0 up to an epsilon corresponding to the maximum ε for which the distribution is bilocal (Fig. 23). The proof can easily generalizes to the case in which p_1 is not deterministic because, as we are in the bilocal set, this p_1 can always be written as a convex combination of deterministic strategies.

As we explained in section 2.1, any bilocal correlation can be represented as in Fig. 24, so every distribution represented in this picture can be factorized as $p_A p_C$. p_1 is a deterministic strategy, i.e. it can be written as $p_1 = \delta(a - A(x))\delta(c - C(z))$, and it is represented

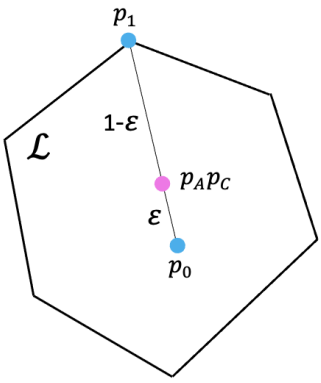

Figure 23: Representation of the convex combination which results in $p_A p_C$ and has a quasi-deterministic strategy. The polygone represents the local set $\mathcal{L}$.

by one of the 16 squares in the figure. Thus, $\varepsilon \equiv p(b = 1)$ corresponds to the coloured area. Knowing that, p_0 can be constructed as:

$$p_0 = \frac{p_A p_C - \varepsilon p_1}{1 - \varepsilon}. \tag{62}$$

ε can be increased up to a limit that corresponds to the maximum area that the square

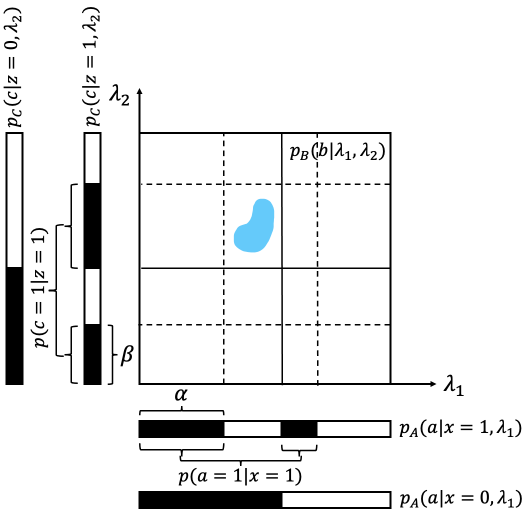

Figure 24: Representation of a bilocal correlation where the coloured part ($p(a, b = 1, c|x, z)$) corresponds to a deterministic strategy.

representing the deterministic strategy p_1 can have, which corresponds to the limit of the bilocal set.

■